


Self-Regeneration of Pd–LaFeO₃ Catalysts: New Insight from Atomic-Resolution Electron Microscopy

Michael B. Katz,[†] George W. Graham,[†] Yingwen Duan,[†] Hong Liu,[†] Carolina Adamo,[‡] Darrell G. Schlom,[‡] and Xiaoqing Pan^{*,†}

[†]Department of Materials Science and Engineering, University of Michigan, Ann Arbor, Michigan 48109, United States

[‡]Department of Materials Science and Engineering, Cornell University, Ithaca, New York 14853, United States

 Supporting Information

ABSTRACT: Aberration-corrected transmission electron microscopy was used to study atomic-scale processes in Pd–LaFeO₃ catalysts. Clear evidence for diffusion of Pd into LaFeO₃ and out of LaFe_{0.95}Pd_{0.05}O_{3–δ} under high-temperature oxidizing and reducing conditions, respectively, was found, but the extent to which these processes occurred was quite limited. These observations cast doubt that such phenomena play a significant role in a postulated mechanism of self-regeneration of this system as an automotive exhaust-gas catalyst.

Automotive exhaust-gas catalysts require a substantial fraction of the world's supply of Pt, Pd, and Rh.¹ The fraction would be lower, however, if the nanometer-sized metal particles present in a fresh catalyst could be stabilized against growth during use. A Pd–perovskite catalyst formulation has previously been found to maintain an unusually high level of activity upon aging,² and an ingenious process of self-regeneration, involving cyclical dissolution and segregation of Pd into and out of the perovskite lattice during normal use, was proposed by Nishihata et al. to account for its stability.³ Though appealing,^{4–6} this explanation, which is based largely on XANES and EXAFS measurements, has not been verified via direct examination of catalyst dispersion. Here we present results from our atomic-resolution transmission electron microscopy (TEM) study that cast doubt on the viability of the self-regeneration concept.

Our study, which follows up on the Nishihata et al. proposal regarding self-regeneration, focuses primarily on a model planar catalyst geometry that is ideally suited to cross-sectional TEM techniques. Initially, we considered Pd-doped LaFeO₃, LaFe_{0.95}Pd_{0.05}O_{3–δ}, following the lead of Tanaka et al., who prepared such a composition in high-surface-area powder form to represent the fresh state of their ultimate 'intelligent catalyst'.⁷ In our work, thin (thickness on the order of 100 nm) single-crystal films were grown epitaxially on (100) SrTiO₃ substrates using pulsed-laser deposition (PLD), and samples were subjected to various thermal treatments under flowing gas mixtures in a quartz tube furnace. Changes in surface composition induced by thermal treatment were determined by X-ray photoelectron spectroscopy (XPS), and TEM cross-sectional specimens were subsequently prepared.

Examination of the as-grown film by TEM revealed an atomically flat, well-ordered crystalline surface, and XPS found the expected surface composition. Two distinct chemical states of

Pd, both ionic but neither corresponding to the usual +2 state in PdO, were also observed by XPS, whereas Tanaka et al. reported only the combination,⁷ possibly due to a lower instrumental energy resolution. Following a reduction treatment (1% H₂ in N₂ at 600 °C for 1 h), the state at relatively higher binding energy lost some of its intensity; however, unlike the results of Tanaka et al.,⁷ no new state corresponding to metallic Pd appeared, and the overall intensity of the Pd photoemission peaks did not increase relative to that of the other perovskite peaks. An additional reduction treatment at both higher H₂ concentration (5%) and temperature (700 °C) was needed to produce the first indication of any metallic Pd, and only by increasing the H₂ concentration to 10% and the temperature to 800 °C was much of the Pd converted to the metallic state, as shown in Figure 1a.

At this stage, TEM revealed very few Pd particles (surface area density no more than about 10² μm⁻²), each having an average diameter 3 nm, all of which were epitaxial. An example of such a particle is shown in Figure 1b. The observed interfacial structure is consistent with density functional theory, which predicts that bonding of Pd to LaO layers should be preferred.⁸ According to X-ray energy dispersive spectroscopy (EDS) measurements, there was essentially no change in average Pd concentration within the perovskite, indicating that little of the Pd was expelled onto the surface of the film. In fact, the metallic Pd found on the surface in the form of particles after the final reduction treatment corresponds to the amount initially present within just a nanometer of the surface, consistent with the XPS observations. Similar observations were made on high-surface-area powders, although the results are less ambiguous (Appendix A, Supporting Information).

Since we were unable to produce many Pd particles on the surface of these films by the reduction treatment, we adopted an alternative approach to examine the metal-particle dissolution process. Thus, single-crystal films of pure LaFeO₃ were grown on (100) SrTiO₃ substrates, again by PLD. The stoichiometry of these films was not exact, however, there being a deficiency in Fe (Fe:La = 0.85), according to wavelength-dispersive X-ray spectroscopy measurements. Approximately one monolayer of Pd was then deposited onto the film surface by thermal evaporation in ultrahigh vacuum, and samples were again subjected to various thermal treatments under flowing gas mixtures in a quartz tube furnace. As before, changes in surface

Received: September 2, 2011

Published: October 18, 2011

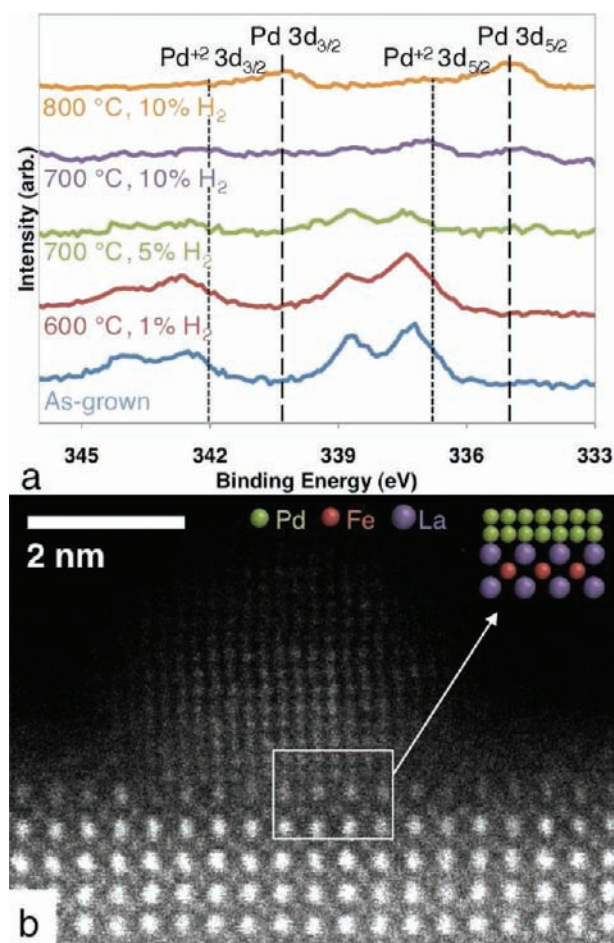


Figure 1. (a) XPS spectra of the $\text{LaFe}_{0.95}\text{Pd}_{0.05}\text{O}_{3-\delta}$ PLD thin film after various thermal treatments. (b) High-angle annular dark-field scanning transmission electron microscopy (HAADF-STEM) image of a typical Pd particle found on the $\text{LaFe}_{0.95}\text{Pd}_{0.05}\text{O}_{3-\delta}$ film surface after the most aggressive reduction step.

composition induced by thermal treatment were subsequently determined by XPS, and TEM cross-sectional specimens were examined after appropriate stages of the treatment.

A low magnification image of the cross section of a sample that was first reduced (1% H_2 in N_2 at 600 °C for 1 h), then oxidized (air at 800 °C for 1 h) is shown in Figure 2a. The initial reduction treatment in this case was intended to stimulate growth of moderately sized Pd particles on the surface prior to oxidation. Although the perovskite surface is not atomically flat, it is clear that the Pd (as PdO) particles have sunk partially into the LaFeO_3 , and a definite reaction zone around the particles can be distinguished by a lower level of contrast relative to the adjacent LaFeO_3 . This phenomenon is illustrated more clearly for the particle at the extreme left side of the image in the enlargement, shown in Figure 2b. The accompanying compositional line scan in Figure 2c, obtained by electron energy loss spectroscopy (EELS), reveals a slight increase in the Fe/La ratio, relative to the adjacent LaFeO_3 , in the portion of the zone just outside the PdO particle (i.e., 3–6.5 nm along the x -axis of the line scan). This variation in composition, confirmed by EDS in several other examples of the zone, provides a clue, although so far not understood, about the detailed nature of the reaction.

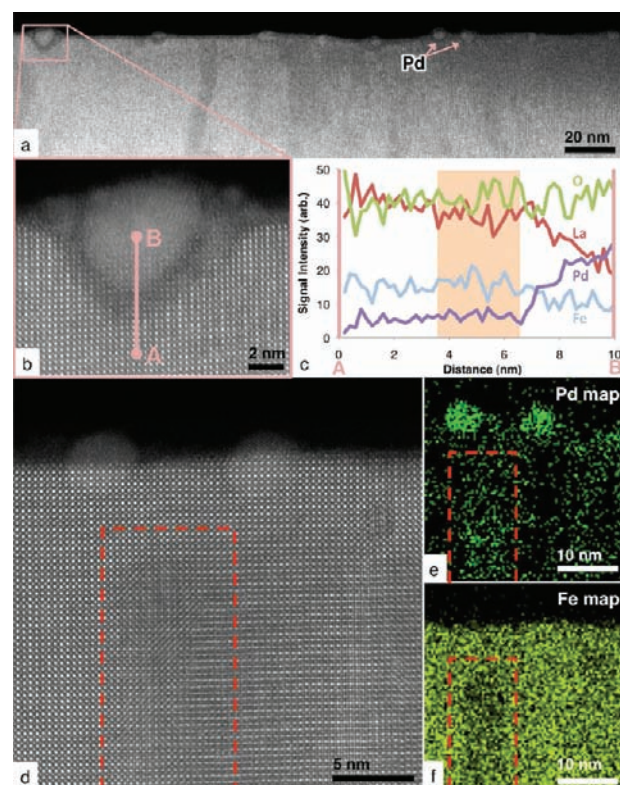


Figure 2. (a) HAADF-STEM image of a typical region of the oxidized Pd/ LaFeO_3 PLD thin film, with (b) an image at higher magnification of one of the partially embedded PdO particles and (c) an EELS line scan taken across the reaction zone at the interface between the oxide and the particle in (b), as indicated by the line A–B. The shaded region in (c) corresponds to the reaction zone in (b). (d) HAADF-STEM image of a region of the oxidized Pd/ LaFeO_3 PLD thin film with a visibly distorted lattice, together with corresponding (e) Pd and (f) Fe EDS maps. The indicated areas contain Pd (at levels estimated to be approximately 20% of Fe) within the oxide.

In addition to this indication of a local reaction between the PdO particles and the perovskite film, EDS mapping revealed the presence of some Pd within the film, as shown in Figure 2d–f. As expected from the work of Nishihata et al., regions with Pd (as indicated) are also regions of relatively low Fe concentration, since Pd is known to take the place of Fe in the perovskite lattice. It seems likely that regions of low Fe concentration were present in the film, as grown, due to its off-stoichiometry. Further, crystal defects indicated by structural disorder are also clearly evident in these regions, possibly providing channels for Pd diffusion. On the basis of a comparison of the EDS signals from the doped film discussed above and from this region, the local Pd concentration here is estimated to be about 20% of the Fe concentration.

In order to gauge the importance of crystal defects (including Fe vacancies) in allowing Pd to enter the film well below its surface, we also considered pure LaFeO_3 films (made by molecular beam epitaxy [MBE]), which are of much higher crystalline quality than the PLD films. Figure 3a shows a cross-sectional image obtained from such a sample, which was simply oxidized (air at 800 °C for 1 h) after Pd was deposited onto its surface. Again, there is clear indication of a local reaction between the PdO particles and the film, as in the case of the PLD film, but the concentration of Pd within the film was much lower

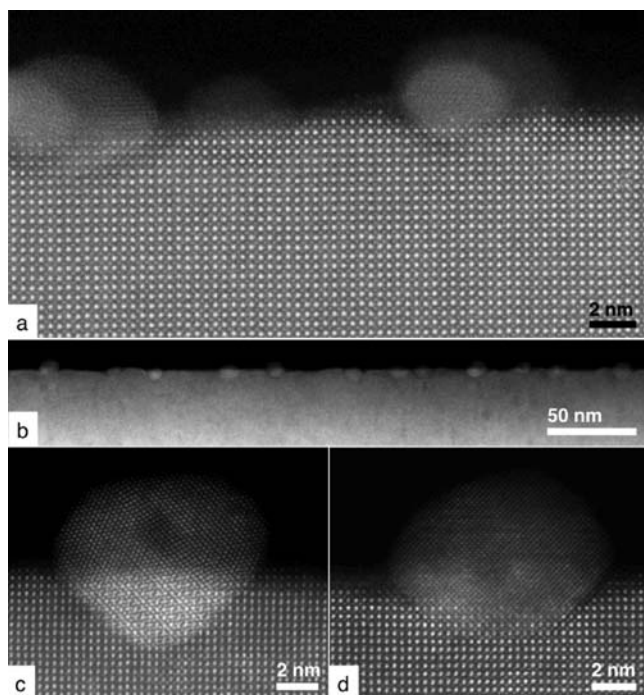


Figure 3. (a) HAADF-STEM image of a typical surface region of the oxidized Pd/LaFeO₃ MBE thin film. Note that Pd particles have again reacted with the oxide, sinking partially into the surface. (b) HAADF-STEM image of a typical area on a Pd/LaFeO₃ MBE film after 10 h of redox cycling at 600 °C and (c, d) two typical Pd particles shown in detail, with the particle in (d) being epitaxial.

(i.e., below the detection limit of EDS). We conclude that the crystalline quality of LaFeO₃ is not a determining factor in the local reaction that occurs around individual PdO particles contacting the perovskite film, but that the presence of certain types of defects may be necessary for much Pd to diffuse from the surface into the bulk of the perovskite film under oxidizing conditions.

To ascertain the effects of extended catalyst operation (involving alternate exposure to both oxidizing and reducing conditions) on Pd dispersion and coarsening, we subjected Pd-coated LaFeO₃ MBE thin films, initially oxidized as above, to mild redox cycling (heating to 600 °C in N₂ followed by alternating 10-min periods of 1% H₂ or 0.5% O₂ in N₂ for 10 h total, followed by cooling in 0.5% O₂ in N₂). The Pd particles on the surface were generally 5–10 nm in diameter, and all were found to be partially embedded in the support surface, as can be seen in Figure 3b. Many of the particles exhibited some degree of epitaxial registration with the perovskite; two typical examples are shown in Figure 3c,d. While the support no longer had an atomically flat surface, the LaFeO₃ showed no obvious signs of deterioration. The morphology induced by the initial oxidation treatment is thus stable under extended redox cycling. This situation may be contrasted with that in other more typical supports, such as CeO₂, where Pd particles remain entirely on the surface (Appendix B, Supporting Information).

To summarize our observations, it appears that both the formation of Pd particles on the surface of Pd-doped LaFeO₃ under reducing conditions as well as the dissolution of Pd particles into LaFeO₃ under oxidizing conditions are much more

limited processes than we would have expected on the basis of results from Nishihata et al. (i.e., complete exchange of Pd within 1 h at 800 °C), even in the case of the somewhat defective PLD films. Whereas the diffusion of Pd (as ions) very far beneath the perovskite surface likely requires large numbers of defects (possibly both Fe vacancies as well as other extended types such as point defect clusters, threading dislocations, and orthorhombic twinning boundaries), the strong reaction between Pd (or PdO) particles and LaFeO₃ that occurs locally under oxidizing conditions is independent of LaFeO₃ crystalline quality. In fact, the length scales observed in these two instances, 100 and 1 nm, are consistent with grain boundary and bulk cation diffusion (distance $\approx (Dt)^{0.5}$, where D is the cation diffusion constant and t is the time), respectively, in LaFeO₃.⁹

While we confirm that processes proposed by Nishihata et al. occur to a very limited extent, the predominant mode, according to our observations, is the localized reaction that occurs between Pd particles situated on the surface and the perovskite support under oxidizing conditions. The surface morphology induced by this predominant mode (i.e., that shown in Figure 3b), which we confirmed also persists under our most aggressive reducing condition (10% H₂ in N₂ at 800 °C for 1 h), has itself previously been connected with increased particle stability: particles sitting in cavities (in this case, generated by the particles themselves) are more resistant to growth due to processes involving both interparticle transport and particle migration than particles sitting on a flat surface, assuming the same contact angle in both cases.¹⁰

Finally, we comment on the connection between our main results and those of Nishihata et al. By way of justification for such a comparison, we note that the perovskite particles in the powder form of this catalyst are typically characterized by a dimension that is similar to the minimum dimension of our thin films, 100 nm, and that they appear to be simply crystalline in nature, i.e., contain few extended defects (Appendix A, Supporting Information). Thus, the film and powder forms are structurally quite similar. But how, then, can one account for the XANES and EXAFS results of Nishihata et al. (and others)? We have recently shown that reversible precipitation/redissolution of precious metal-rich clusters occurs throughout the interior of the perovskite film under reducing/oxidizing conditions in other systems that are also considered ‘intelligent catalysts’.¹¹ The perovskite materials in these systems are also crystalline, and the distance over which the precious metal ions move is only a few nanometers, consistent with expectations based on diffusion data, just as in the Pd–LaFeO₃ system. While we cannot image such clusters in the Pd–LaFeO₃ system, we suspect they may also form. If so, the reversible formation and disappearance of such clusters could well account for the XANES and EXAFS results in a way that is largely irrelevant for catalysis.

■ ASSOCIATED CONTENT

S Supporting Information. Materials, methods, experimental details, and appendices with additional information. This material is available free of charge via the Internet at <http://pubs.acs.org>.

■ AUTHOR INFORMATION

Corresponding Author

panx@umich.edu

ACKNOWLEDGMENT

The work at the University of Michigan was supported by the National Science Foundation under Grants DMR-0907191, CBET-0933239, and DMR-0723032. The work at Cornell University was supported by ARO through agreement W911NF-08-2-0032. We acknowledge M. Kawasaki, E. Okunishi, and D. Blom for technical assistance using aberration-corrected TEMs, K. Sun for technical assistance using the XPS instrument, C. Henderson for obtaining the wavelength-dispersive X-ray spectroscopy results, and also H.-W. Jen for performing the extended cyclical redox treatment.

REFERENCES

- (1) Butler, J. *Platinum 2010 Interim Review*; Johnson Matthey: London, 2010.
- (2) Tanaka, H.; Fujikawa, H.; Takahashi, I. Perovskite-Pd Three-Way Catalysts for Automotive Applications. *SAE Technical Papers*; SAE International: Warrendale, PA, U.S.A., 1993; 10.4271/930251.
- (3) Nishihata, Y.; Mizuki, J.; Akao, T.; Tanaka, H.; Uenishi, M.; Kimura, M.; Okamoto, T.; Hamada, N. *Nature* **2002**, *418*, 164–167.
- (4) Li, J.; Singh, U. G.; Bennett, J. W.; Page, K.; Weaver, J. C.; Zhang, J.-P.; Proffen, T.; Rappe, A. M.; Scott, S.; Seshadri, R. *Chem. Mater.* **2007**, *19*, 1418–1426.
- (5) Chiarello, G.; Ferri, D.; Grunwaldt, J.; Forni, L.; Baiker, A. *J. Catal.* **2007**, *252*, 137–147.
- (6) Eyssler, A.; Mandaliiev, P.; Winkler, A.; Hug, P.; Safonova, O.; Figi, R.; Weidenkaff, A.; Ferri, D. *J. Phys. Chem. C* **2010**, *114*, 4584–4594.
- (7) Tanaka, H.; Tan, I.; Uenishi, M.; Taniguchi, M.; Kimura, M.; Nishihata, Y.; Mizuki, J. *J. Alloys Compd.* **2006**, *408–412*, 1071–1077.
- (8) Li, B. H.; Katz, M. B.; Van der Ven, A.; Chen, L.; Graham, G. W.; Pan, X. Q. Manuscript in preparation.
- (9) Waernhus, I.; Sakai, N.; Yokokawa, H.; Grande, T.; Einarsrud, M.-A.; Wiik, K. *Solid State Ionics* **2007**, *178*, 907–914.
- (10) Wynblatt, P.; Gjostein, N. A. *Prog. Solid State Chem.* **1975**, *9*, 21–58.
- (11) Katz, M. B.; Duan, Y. W.; Zhang, S. Y.; Sun, K.; Graham, G. W.; Pan, X. Q. Manuscript in preparation.